Modelling the reactions of cellulose, hemicellulose and lignin submitted to hydrothermal treatment

A.M. M Borrero-López, E. Masson, A. Celzard, V. Fierro

Modelling the reactions of cellulose, hemicellulose and lignin submitted to hydrothermal treatment

A.M. Borrero-López[1], E. Masson[2], A. Celzard[1], V. Fierro[1*]

[1] Université de Lorraine, CNRS, IJL, F-88000 Epinal, France

[2] CRITT Bois, 27 rue Philippe Seguin, BP 91067, 88051 Epinal Cedex 9, France

Abstract

The main compounds of plant biomass, i.e., cellulose, lignin and hemicellulose, were submitted to hydrothermal carbonisation (HTC) in ranges of temperature and time of 140-240ºC and 0.5-24 h, respectively. Those parameters were combined into a single one, the severity factor, and its effect on hydrochar yield on the one hand, and on pH, yield and composition of the liquid fraction on the other hand, was investigated in depth. The production of furanic and phenolic compounds was correlated with both severity and pH. The kinetics of furfural (FU) and 5-hydroxymethylfurfural (5-HMF) production and consumption were also investigated and modelled, and the results were compared to those reported in the literature. The production of nine phenolic compounds from lignin HTC was also considered.

[*] Corresponding author. Tel: + 33 372 74 96 77. Fax: + 33 372 74 96 38. E-mail address : Vanessa.Fierro@univ-lorraine.fr (V. Fierro)

1. Introduction

Hydrothermal carbonisation (HTC), whose history dates from the early 1900's (Bergius, 1915), is a very simple process by which a bioresource is submitted to mild temperatures (130-250ºC) in a pressurised liquid medium (generally pure water) using a closed reactor, i.e., an autoclave. In the latter, the pressure is self-generated and allows obtaining both solid and liquid products (Borrero-López et al. 2017).

HTC is cost-effective as it does not require chemicals and avoids costs related to materials drying, and it perfectly allows biomass conversion into high added-value organic compounds through hydrolysis and subsequent dehydration and fragmentation (Braghiroli et al., 2015). Cellulose, hemicellulose and lignin are the main macromolecular compounds of wood and plant biomass in general, and the former two macromolecules are well-known precursors of furfural (FU) and 5-hydroxymethylfurfural (5-HMF), respectively, when submitted to HTC. HTC of lignin can also provide some valuable compounds like vanillin, used for cosmetics and flavouring, or syringaldehyde, used as ingredient for food and flavour (Onwudili, 2015, Zhou, 2014), amongst others.

However, a solid carbonaceous residue, called hydrochar, is also obtained in the same process, having many interesting features such as porosity and functional groups like hydroxyls, carbonyls, etc (Chen et al., 2017). Hydrochars are interesting by-products as they present higher heating values (Basso et al., 2015) than their corresponding biomass precursors, and have been proposed for soil amendment (Steinbeiss et al., 2009), for CO_2 capture (Jatzwauck and Schumpe, 2015) or as precursors of carbon materials (Borrero-López et al., 2017, Braghiroli et al., 2012, 2015b).

Extensive work has been carried out on HTC of many kinds of bioressources, like wheat straw (Reza et al., 2015), plant biomass wastes (Fang et al., 2015), loblolly pine (Lynam et al., 2011), soft rush (Jatzwauck and Schumpe, 2015) as well as on each

individual major compound of such biomass (Lu et al., 2013, Gao et al., 2012, Pińkowska et al., 2011, Wang et al., 2015). However, only a few works combined the studies of cellulose, hemicellulose and lignin. For instance, Kang et al. (2012) previously focused on HTC of the latter compounds, amongst others, but only a rather narrow temperature range was investigated and no detailed studies of the liquid products was performed. As far as we know, no research related to the liquid and solid fractions obtained from cellulose, hemicellulose and lignin submitted together to HTC has been published.

In the recent past, the kinetics of FU production / decomposition competitive reactions (Marcotullio et al., 2009) were thoroughly studied for several biomasses or biomass-derived molecules such as wheat straw (Yemiş and Mazza, 2012) and xylose (Liu et al., 2014) submitted to HTC. Most works generally focused either on production or on decomposition reactions separately (Liu et al., 2014, Danon et al., 2014, Kim et al., 2011). Simple consecutive reaction models as well as models taking into account side reactions have been developed (Jing and Lü, 2007, Liu et al., 2014) and are in agreement with published studies on degradation compounds from sugars (Rasmussen et al., 2014, Yang et al., 2012, Chen et al., 2012). An intermediate between xylose and furfural has also been proposed for explaining the kinetics of FU production (Marcotullio, 2011 and Chen et al., 2015).

Regarding the kinetics of reaction of 5-HMF, Chen et al. (2010) studied its production whereas Girisuta et al. (2006) studied its decomposition to levulinic acid, but again there was not too much work related with these two competitive processes in the same study (Jing and Lü, 2008, Shen and Wyman, 2012). The case of 5-HMF is more complex than that of FU, because some degradation products are known to decompose afterwards, such as levulinic acid.

The main purpose of the present work was to assess the effect of HTC conditions on lignin, cellulose and hemicellulose in a broad range of temperatures (140-240ºC) and time (0.5-24 hours), by studying the production of FU, 5-HMF and up to nine aromatic compounds as a function of HTC severity, and to apply simple models for describing the observed kinetics. Relationships between the latter and pH, and yields of resultant liquid and solids, were also looked for.

2. Material and Methods

2.1. Raw material

Cellulose was Type 102 VIVAPUR (high-purity) microcrystalline cellulose provided by JRS Pharma (Rosenberg, Germany). Hemicellulose was high-purity xylan extracted from beech wood and supplied from Roth (Karlsruhe, Germany). Lignin used was lignin powder Lignine PROTOBIND 1075 (Asian Lignin Manufacturing India Private Limited), which is soda lignin. All compounds used for identification and quantification of phenolic and furanic compounds by HPLC were analytical grade and purchased from Sigma-Aldrich (Steinheim, Germany).

2.2. Hydrothermal carbonisation (HTC)

HTC experiments were performed in 100 mL Teflon®-lined autoclaves. The liquid to solid (L/S) weight ratio was 8 (16 g / 2 g) where L stands for liquid (i.e., pure water) and S for the considered biomass compound (BC) on dry basis. BC and distilled water were thus weighed and introduced in a glass insert so as to protect the PTFE liner of the autoclave from any contamination. Autoclaves were next hermetically closed and placed in a ventilated oven preheated at the desired temperature (160, 170, 180, 200, 220 or 240ºC) for the required reaction time (from 0.5 to 24 hours). Afterwards, the

autoclaves were removed from the oven and let to cool down to room temperature for several hours before opening.

Since both time (t) and temperature (T) produce changes in the results of the HTC process, their effect was investigated through the severity factor ($\log R_0$) which was introduced to combine these two parameters into a single one (Overend and Chornet, 1987). Indeed, $\log R_0$ takes into account the different significances of these two parameters through an exponential factor for the temperature, and through a proportional factor for time. It reads:

$$logR_0 = \log\left[t \cdot \exp\left(\frac{T-100}{\omega}\right)\right] \quad (1)$$

where t is the residence time (min), T the working temperature (°C) and ω is an HTC parameter. The initial value for lignocellulosic materials that was suggested for ω was 14.75, since it corresponds to the activation energy of a first-order hydrolytic process (Xu et al., 2011). As it remains an empirical parameter, ω was sometimes changed when using other bioresources and different temperature ranges, as did Ko et al. (2015) for glucose by using the value 4.6.

2.3. Liquid/solid separation and analysis

After HTC, liquid and solid products obtained together in the autoclave were separated by vacuum filtration. The amount of liquid was weighed immediately after filtration, whereas solids were placed in a vacuum oven for 6 hours at 60ºC for complete drying and subsequent weighing.

Qualitative identification of the main volatile compounds in the liquid phase was carried out by gas chromatography coupled with mass spectrometry (Clarus 500 GC/MS). Regarding quantitative analyses, furanic and phenolic compounds were

determined using an Ultimate 3000 high-performance liquid chromatograph equipped with auto-sampler, diode array and fluorescence detectors, and columns described below.

A Hypersyl Green PAH column was used for FU, 5-HMF and 5-MF quantification. Four UV absorption wavelengths were used, i.e., 220, 276, 284 and 291 nm. Doing so, fluorescence and emission occurring at wavelengths of 360 nm and 443 nm, respectively, could be avoided. Water and acetonitrile were used as mobile phases and the acetonitrile/water ratio was changed from 5/95 to 100/0 during the 35 min of the total analysis time as follows: in the first 1.5 min, the 5/95 ratio was maintained; from 1.5 to 15min, acetonitrile increased linearly up to a 50/50 ratio; from 15 to 20 min, the acetonitrile again increased up to 100/0 and this ratio was maintained for 5 min more. From 25 to 30 min, acetonitrile decreased until the initial ratio, i.e., 5/95, and it was maintained 5 min until the end of the analysis.

Phenolic compounds were quantified with a Pinnacle DB BiPh 5µm column, and UV absorption wavelengths of 195, 201, 231 and 300 nm were used. Mobile phases were water and acetonitrile too. The program started with an acetonitrile/water ratio of 10/90 during the first 3 min. Later, the acetonitrile content increased up to 15/85 at min 5, and remained constant until min 13. From 13 to 15 min, acetonitrile increased up to the ratio 20/80 and was kept constant 13 min more. From 28 to 33 min, the acetonitrile concentration increased up to the ratio 100/0, which was kept for 5 min more. From 38 to 43 min, acetonitrile concentration decreased to 90/10 ratio, and remained constant for 7 min more, until the end of the experiment at 50 min. Again, all the aforementioned changes of the acetonitrile/water ratio were linear.

The yield of each considered organic molecule X, Y_X, was calculated according to the following equation:

144 $$Y_X\ (\%) = \frac{[X]\,V}{W_{BC}} \times 100 \quad (2)$$

145 where $[X]$ is the concentration (g mL^{-1}) of each soluble organic compound within the
146 volume V of liquid (mL) obtained after HTC, and W_{BC} is the mass (g) of the biomass
147 component studied on dry basis.

148 The hydrochar yield, Y_{HC}, was determined from Eq. (3):

149 $$Y_{HC}\ (\%) = \frac{W_{HC}}{W_{BC}} \times 100 \quad (3)$$

150 where W_{HC} is the mass of dry hydrochar after HTC.

151 The liquid yield from HTC, LY_{HC}, was calculated as follows:

152 $$LY_{HC}\ (\%) = \frac{LW_{HC}}{LW_0} \times 100 \quad (4)$$

153 where LW_{HC} is the amount of liquid weighed after filtration, and LW_0 is the initial
154 amount of liquid added in the autoclave.

155

156 **2.4. Kinetics**

157 The fits to experimental kinetic data was carried out with OriginPro 8.5.1 software
158 by minimising χ^2 through the Levenberg-Marquart algorithm. Simple models
159 considering successive decomposition reactions either without or with side reactions,
160 herein called A and B models, respectively (Perez and Fraga 2014, Marcotullio, 2011)
161 were applied to the data, and allowed deriving kinetic parameters for each temperature
162 and for each raw material. The as-obtained kinetic parameters were investigated as a
163 function of temperature using Arrhenius equation, Eq. (5). Both activation energy (E_a)
164 and pre-exponential factor (k_0) were obtained from the slope and intercept of the
165 corresponding fitting, respectively.

166 $$k = k_0\, e^{-\frac{E_a}{RT}} \quad (5)$$

3. Results

3.1. Changes of pH

HTC of cellulose, lignin and hemicellulose produced some changes in the pH of the water in which the process was carried out. Different behaviours were observed, depending on the raw material and on the conditions of the experiments.

Thus, for hemicellulose, the pH first decreased with time (Fig. 1a) likely due to the production of significant amounts of small acidic molecules. Then, the pH either remained low or increased afterwards at higher reaction time, depending on the temperature. Such behaviour is more clearly seen when the pH is plotted versus severity (Fig. 1b), i.e., once time and temperature have been combined into one single parameter. The pH thus increased above a severity of 5, probably because more severe conditions produced secondary reactions which led to the decomposition of low molecular-weight acids as already observed elsewhere (Shen et al., 2012). It might be *a priori* thought that FU and 5-HMF account for the decrease of pH of the solutions recovered after HTC of hemicellulose and cellulose, respectively, since they are generally found at the highest concentrations when the pH decreased the most. However, as furfural is not acidic and 5-HMF possess a pK_a of 12.82, the conditions of their formation at highest concentration may be responsible of the production of other species such as acetic acid, furoic acid, formic acid, lactic acid, propionic acid, butyric acid and others (Zeitsch, 2000, Reza et al., 2014), which really account for the low pH observed.

Roughly similar trends were found when cellulose was submitted to HTC (Fig. 1c), i.e., the pH was the highest at the beginning of the process then decreased and stabilised or slightly increased after 6 – 12h, depending on the temperature. The pH dropped more at higher temperature, but also increased more after the minimum. This trend can be

again explained in terms of increased degradation of soluble products when the severity increased (Fig. 1d), and the apparently constant pH at lower HTC temperature is likely due to reaction times that were too low for causing any significant change of pH.

As for lignin submitted to HTC, the pH of the liquid phase increased with severity (Fig. 1f). This is due to the fact that lignin degradation mainly produces phenolic (i.e., basic) compounds, and not acids. The red solid lines in Fig. 1b, 1d and 1f are fits of a second-order polynomial, Eq. (6), to the experimental data, where p_1, p_2 and p_3 are adjustable parameters. The values of the latter are given in Table 1.

$$Final\ pH = p1 + p2\ (logR_0) + p3\ (logR_0)^2 \quad (6)$$

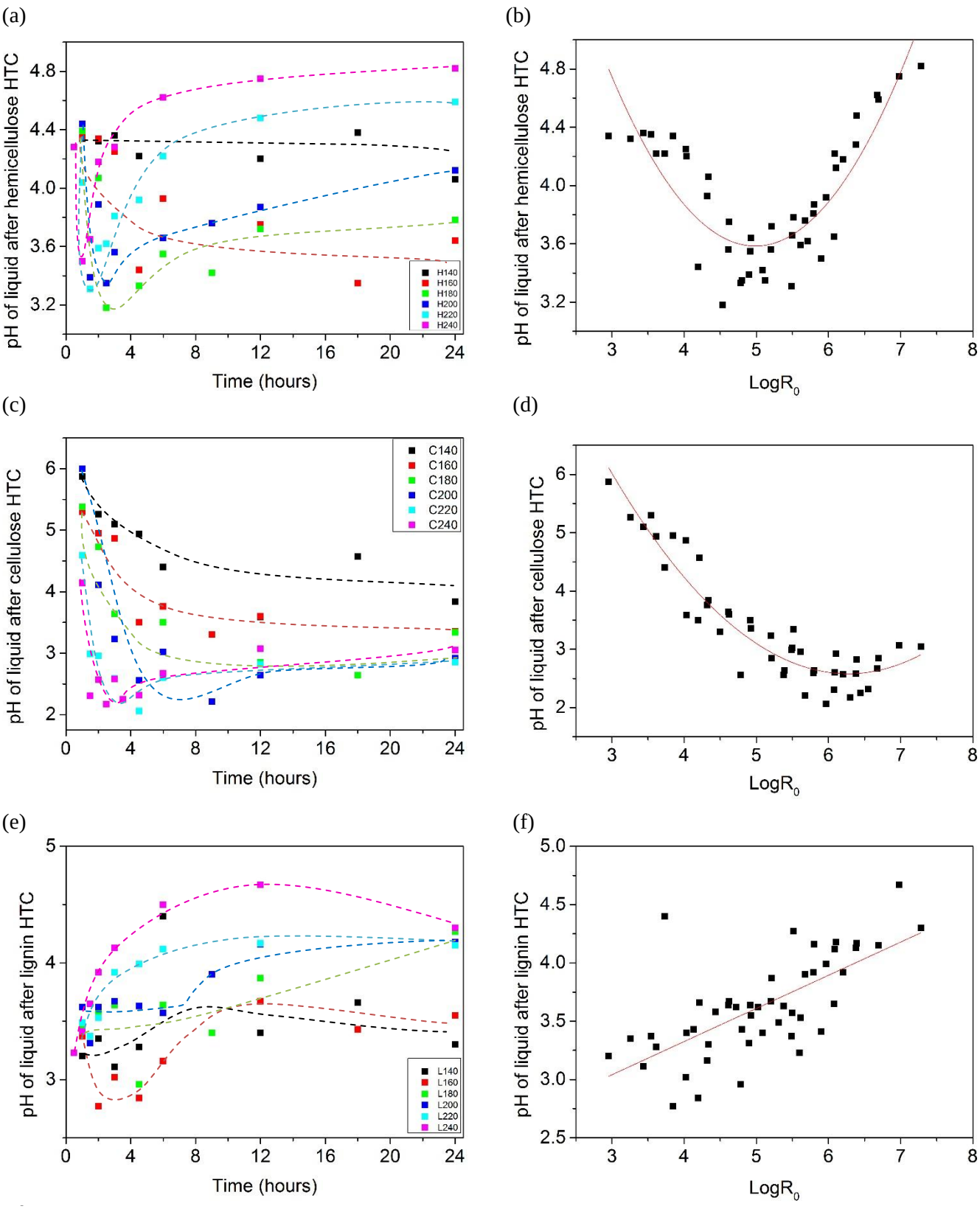

202 Figure 1. Final pH of liquid fractions as a function of time and temperature (left row),
203 and as a function of severity (right row), measured after HTC of: (a) and (b)
204 hemicellulose; (c) and (d) cellulose; (e) and (f) lignin.

Table 1. Values of the parameters of Eq. (6) after fitting the data of Fig. 1b, 1d and 1f.

Biomass component (BC)	p_1	p_2	p_3
Cellulose	15.20	-4.04	0.32
Lignin	2.19	0.28	-
Hemicellulose	10.90	-2.94	0.29

3.2. Yield to hydrochar

The hydrochar yield from hemicellulose ($Y_{HC,H}$) at high severity was lower than that of cellulose and lignin (compare Fig. 2a, 2c and 2e), and the corresponding weight loss also occurred at much lower severity. The yield was indeed around 35% above a severity of 4.5 – 5, and roughly stabilised for higher severity values (Fig. 2a). It is also possible that the curve goes through a minimum at a severity close to 5, as suggested by Fig. 2b showing a slight maximum of liquid fraction, but the natural scattering of the data doesn't allow any firm conclusion about this. Moreover, solid and liquid yields are not necessarily directly related with each other since hydrochars may have retained water bound to their structure, and gases may also have formed (see next subsection).

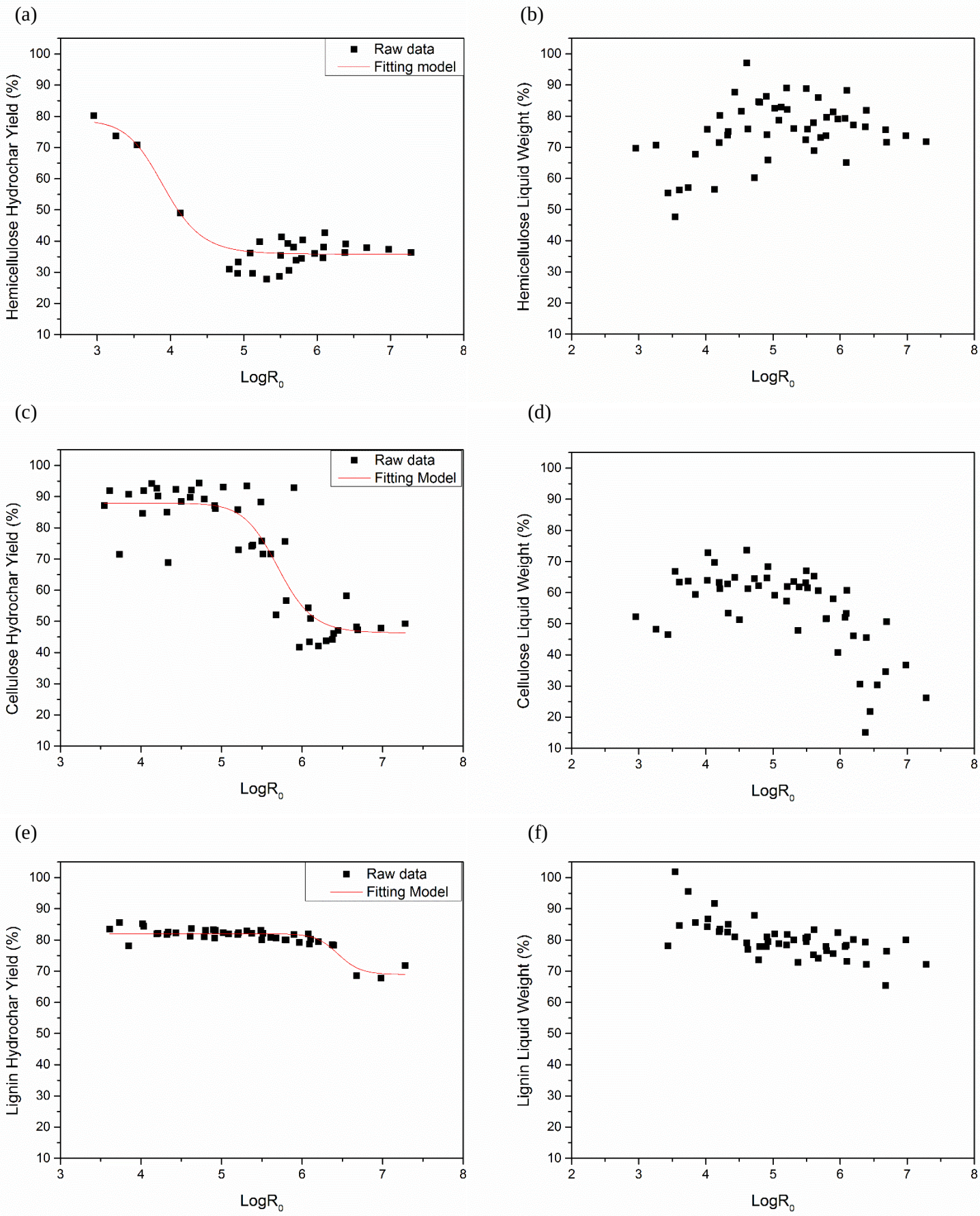

218 Figure 2. Yields of hydrochar (left row) and of liquid fraction (right row) as a function of
219 severity, measured after HTC of: (a) and (b) hemicellulose; (c) and (d) cellulose; (e) and
220 (f) lignin. The red lines are fits of Eq. (7) to the experimental data.

At low severity, cellulose produced the highest amount of HC since the yield was as high as 88%, on average. The weight loss stabilised around 46% at a severity around 6.5, i.e., higher than for hemicellulose. Moreover, the weight loss really started at a severity above 5.5, whereas hemicellulose lost weight from the mildest conditions. This finding is explained by the higher stability of cellulose that remained almost intact until 220ºC, above which degradation began (Fig. 2c).

Lignin was also quite stable since the HC yield was around 81% at low severity, on average, and remained constant up to temperature and time as high as 220ºC and 12h, respectively, corresponding to a severity close to 6.5 (Fig. 2e). Such a yield is a bit lower than that of cellulose in the same conditions because part of the lignin is soluble in water (Overend and Chornet, 1987). Anyway, a lower weight loss than for the previous BCs was observed beyond a severity of 6.5 and quickly seemed to stabilise to around 69%, which was the highest value of the 3 BCs in the most severe conditions.

A kinetic model able to account for the aforementioned trends was applied to the data of Fig. 2a, 2c, and 2e. This model, known as Cross model (Cross, 1965) and described by Eq. (7), has been extensively applied to rheological studies but, to the best of our knowledge, it is the first time that it is applied to hydrothermal carbonisation. It reads:

$$Y_{HC,BC} = \frac{Y_0 + Y_\infty (k\,S)^m}{1 + (k\,S)^m} \qquad (7)$$

where $Y_{HC,BC}$ is the hydrochar yield at a given severity, Y_0 and Y_∞ are the initial and final hydrochar yields, and m and k are parameters accounting for both the slope of the yield drop and the severity value at which the drop starts, respectively. The red lines in Fig. 2a, 2c and 2e show the fits of Eq. (7) to the experimental data. The corresponding adjustable parameters are given in Table 2 for hemicellulose, cellulose and lignin. This

table also includes the coefficient of determination for the three raw materials, demonstrating the good fitting despite the data scattering.

Table 2. Values of the parameters of Eq. (7) after fitting the data of Fig. 2a, 2c and 2e.

Raw material	Y_0 (%)	Y_∞ (%)	k	m	R^2
Hemicellulose	77	35	0.25	21.33	0.89
Cellulose	88	46	0.17	26.42	0.77
Lignin	81	69	0.16	46.46	0.79

3.3. Yield to liquid phase

As observed in Fig. 2, the yields of solid and liquid phases are not strictly correlated with each other. On the one hand, the amount of liquid produced should increase because of the loss of water from biomass but, on the other hand, volatile compounds are likely to be released in the gas phase.

Concerning hemicellulose, the decrease of HC yield was related to the increase of liquid yield until a severity around 5, and the latter remained constant or decreased very slightly at higher severity (Fig. 2b), suggesting that no or negligible amount of gas was produced. When cellulose was submitted to HTC, the liquid fraction was initially roughly constant until a severity of 5.5, above which it decreased very significantly (Fig. 2d). Since the hydrochar yield also decreased, it can be deduced that more and more gas was produced when the conditions turned more severe. As for lignin, the liquid fraction decreased rather linearly with severity over the whole investigated range (Fig. 2f), suggesting that lignin degradation produced volatile compounds from the very beginning, and all the more so at higher severity, as expected.

3.4. FU and 5-HMF production

The production of FU and 5-HMF as a function of HTC time followed the same behaviour, whatever the biomass compound investigated. Thus, at the lowest temperature, FU and 5-HMF production increased monotonously with time. When the HTC temperature increased, a peak of production clearly appeared and was shifted to lower reaction times. Therefore, at the highest investigated temperature, the highest concentration of FU and 5-HMF was obtained in less than 1 h. All these features are shown in Fig. 3. Those trends were more complex than the ones observed above for the changes of pH and yields of hydrochar and liquid fraction, hence the production of FU and 5-HMF as a function of severity were much more scattered than in Fig. 1 and 2. However, a peak of production was still visible in the range of severity 3.5 – 4.5. Fig. 4 shows the example of FU production from cellulose, hemicellulose and lignin.

According to Fig. 3 and 4, the highest concentration peak of FU was obtained from hemicellulose, followed by cellulose and, far behind, lignin. On the contrary, the peak of 5-HMF concentration was the highest for cellulose, followed by hemicellulose and finally lignin (see again Fig. 3). These results are logical since the precursors of FU and 5-HMF are xylans and glucoses, respectively, as they are the main structural units of hemicellulose and cellulose, respectively. FU and 5-HMF production from lignin was thus not expected, and might be due to remaining polysaccharides present as impurities.

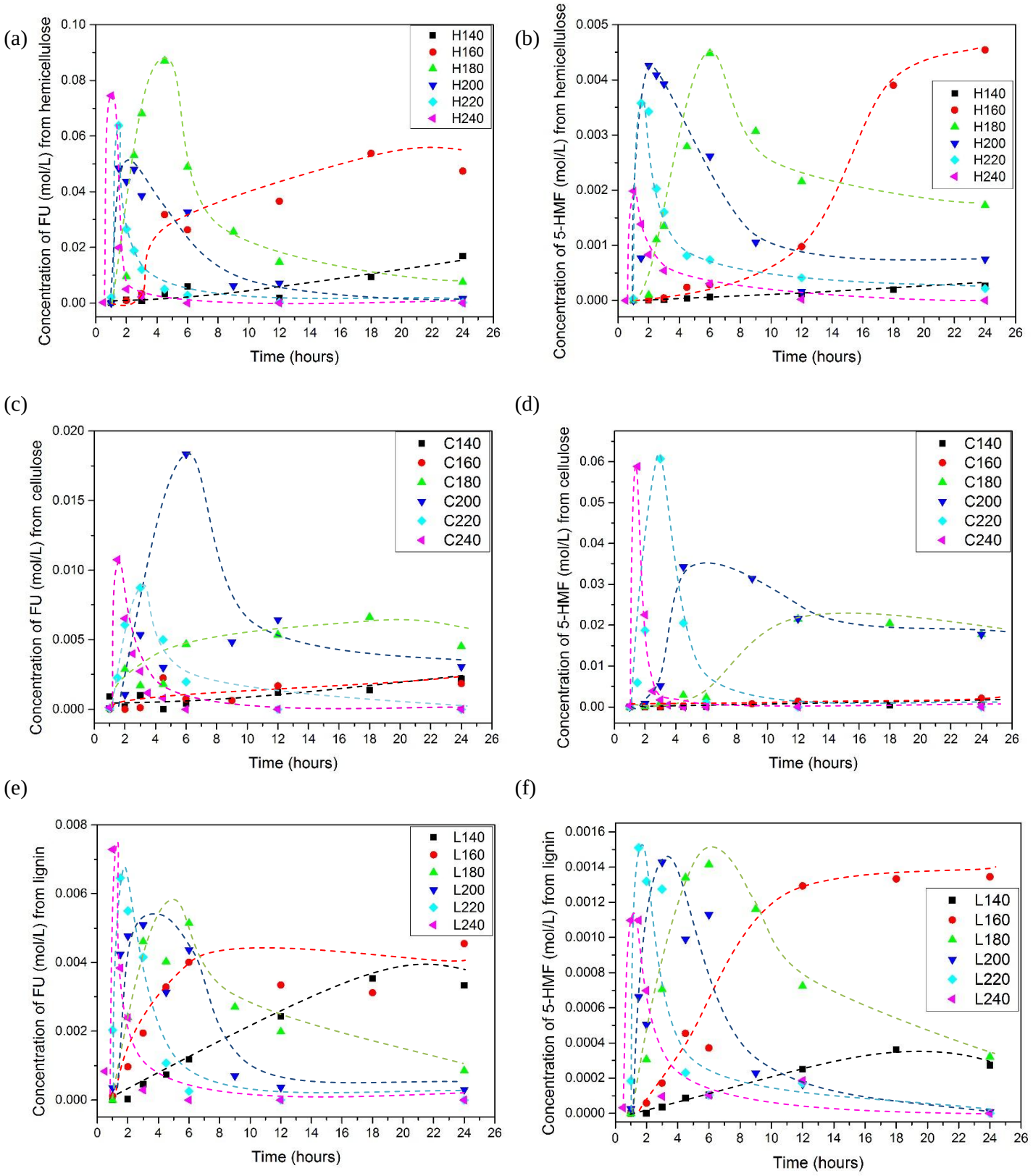

Figure 3. Molar concentration of FU (left row) and 5-HMF (right row) as a function of reaction time, measured after HTC of: (a) and (b) hemicellulose; (c) and (d) cellulose; (e) and (f) lignin.

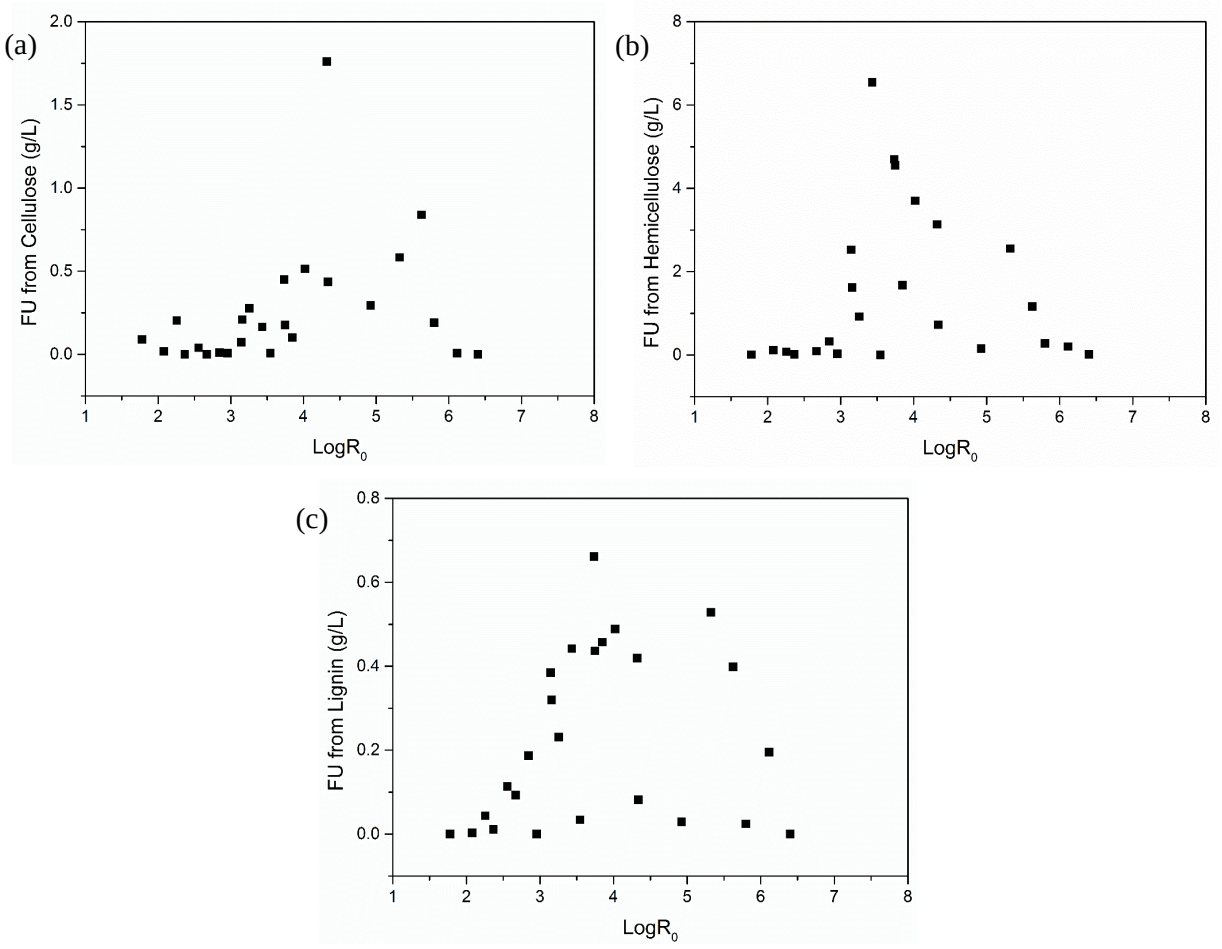

Figure 4. Production of FU by HTC of: (a) cellulose, (b) hemicellulose; and (c) lignin, as function of severity.

3.5. Reaction kinetics

During HTC, FU and 5-HMF were produced but disappeared due to various decomposition reactions. Two different models taking into account consecutive reactions were considered in order to fit the kinetics of both production and decomposition reactions.

The first one, referred to as model A in the following, considers FU and 5-HMF as intermediates between simple sugars derived from BCs and final products, whether those BCs are hemicellulose, cellulose or lignin. All reactions were assumed to be first-order and are presented in Fig. 5 for FU and 5-HMF, respectively.

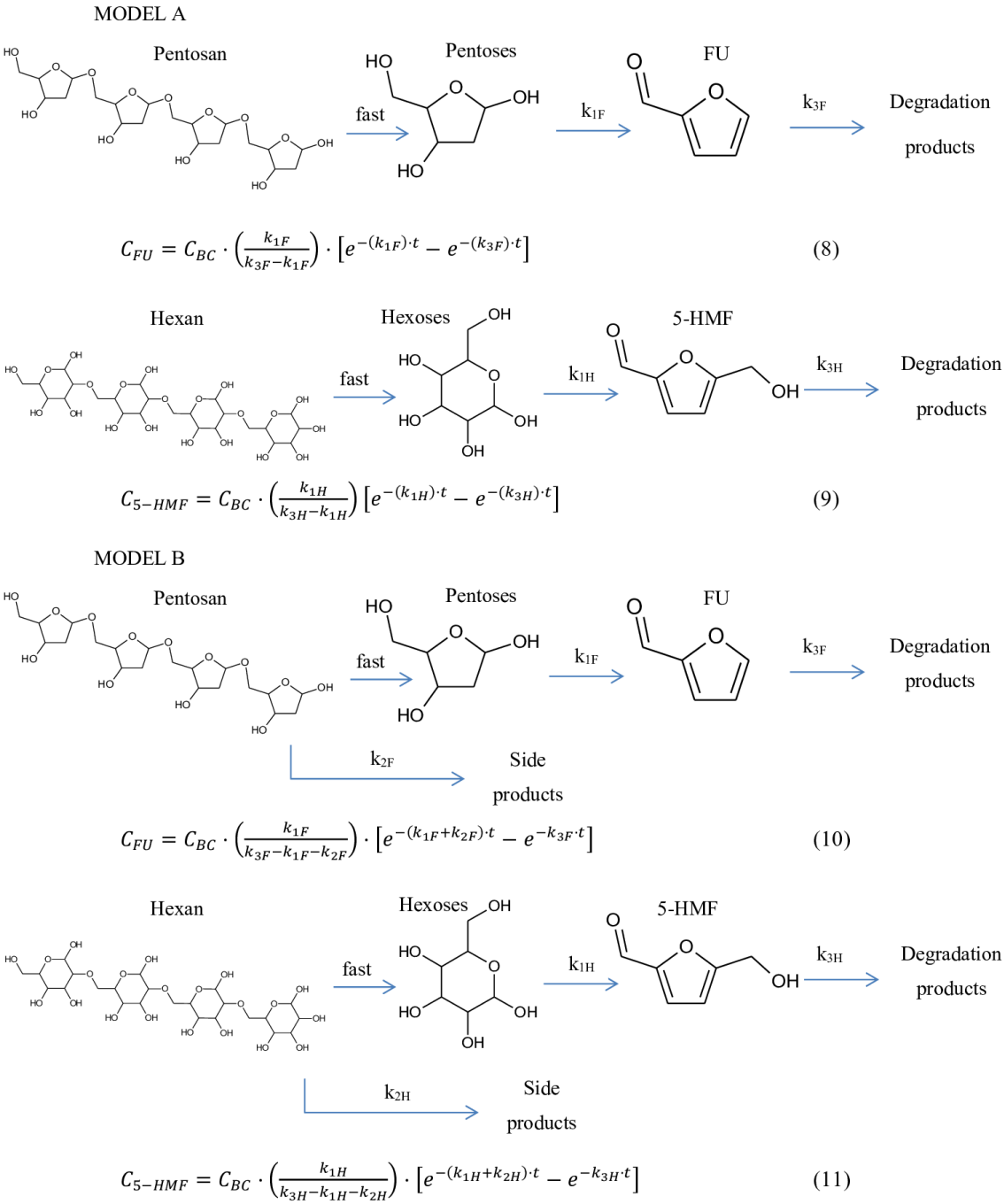

$$C_{FU} = C_{BC} \cdot \left(\frac{k_{1F}}{k_{3F}-k_{1F}}\right) \cdot \left[e^{-(k_{1F})\cdot t} - e^{-(k_{3F})\cdot t}\right] \quad (8)$$

$$C_{5-HMF} = C_{BC} \cdot \left(\frac{k_{1H}}{k_{3H}-k_{1H}}\right) \left[e^{-(k_{1H})\cdot t} - e^{-(k_{3H})\cdot t}\right] \quad (9)$$

$$C_{FU} = C_{BC} \cdot \left(\frac{k_{1F}}{k_{3F}-k_{1F}-k_{2F}}\right) \cdot \left[e^{-(k_{1F}+k_{2F})\cdot t} - e^{-k_{3F}\cdot t}\right] \quad (10)$$

$$C_{5-HMF} = C_{BC} \cdot \left(\frac{k_{1H}}{k_{3H}-k_{1H}-k_{2H}}\right) \cdot \left[e^{-(k_{1H}+k_{2H})\cdot t} - e^{-k_{3H}\cdot t}\right] \quad (11)$$

Figure 5. Models A and B Governing pentoxan and hexan reactions. Model B takes into account competitive reactions to give side products, other than FU and 5-HMF.

The second model, called model B, considers, in addition to the same aforementioned successive reactions, the existence of side reactions leading to the production of other species. In this case, all reactions were assumed first-order too. Side reactions were suggested by Liu et al. (2014), who showed that better fits to the kinetics

311 data were obtained compared to the case of the simple model of consecutive reactions
312 (model A). In other studies, an intermediate compound for each process has been
313 postulated, but could never be isolated or identified (Marcotullio, 2011). Model B,
314 taking into account side reactions, is also sketched in Fig. 5.

315 Herein, it is considered that pentosan directly gives furfural and that hexan gives 5-
316 HMF with kinetic constants k_{1F} and k_{1H}, respectively. FU and 5-HMF decompose to
317 final products with kinetic constants k_{3F} and k_{3H}, respectively. Pentosan and hexan also
318 react by side reactions with constants k_{2F} and k_{2H}, respectively. After resolution of the
319 corresponding differential kinetics equations, FU and 5-HMF concentrations can be
320 expressed by Eq. (8) and (9) for model A, respectively, and by Eq. (10) and (11) for
321 model B, respectively. In those equations, C_{FU}, $C_{5\text{-}HMF}$ and C_{BC} are the initial
322 concentrations of FU, 5-HMF and BC (cellulose, hemicellulose or lignin). Having in
323 mind that xylans and glucoses are the main structural units of hemicellulose and
324 cellulose, respectively. We assumed that BCs decomposed following exclusively model
325 A or model B. This assumption could be less logic for lignin but it is necessary to take
326 into account that here, the fraction of lignin considered is that giving FU and 5-HMF
327 and corresponding to polysaccharides present in lignin as impurities. As it was seen in
328 Fig. 2e, lignin produced more hydrochar, in the whole range of severities tested, than C
329 and H because L is an aromatic molecule prone to condensate as it happens with other
330 polyphenolic compounds as tannins (Braghiroli et al., 2014, 2017, Selmi et al., 2018).

331 By application of these two models, the different constants were obtained, and
332 activation energy (E_a) and pre-exponential factor (k_0) were also determined by
333 application of Arrhenius' Eq. (5) to each kinetic constant. Examples of those Arrhenius
334 fits can be seen in Fig. 6.

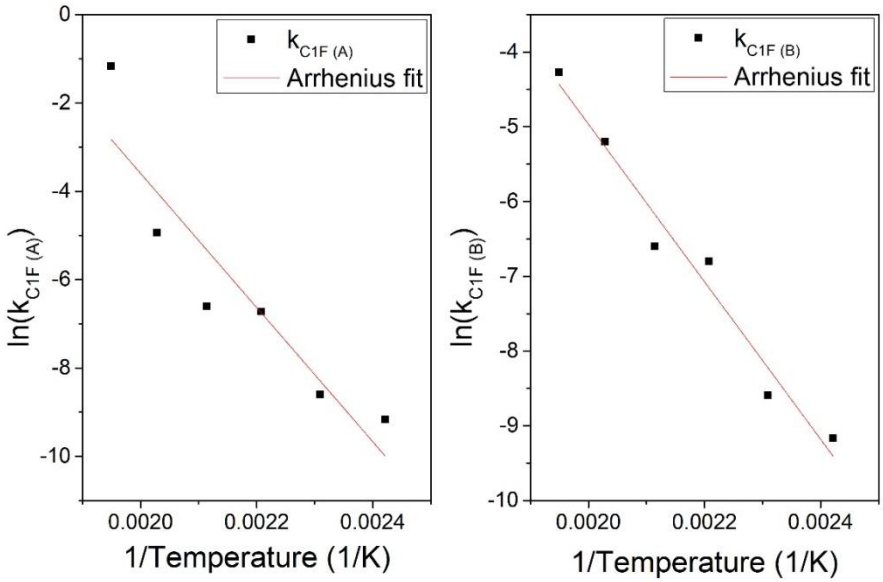

Figure 6. Examples of Arrhenius fitting applied to kinetic constants for cellulose.

Table 3. Activation energy (E_a, kJ·mol^{-1}) and pre-exponential factor (k_0, s^{-1}) for each FU and 5-HMF reaction constant in models A and B.

	Hemicellulose		Cellulose		Lignin	
	Model A	Model B	Model A	Model B	Model A	Model B
FU						
$k_{0,1F}$	2.68E+7	2.93E+4	1.18E+8	2.69E+03	1.87E+10	5.94E+01
$E_{a,1F}$	109.52	85.48	126.25	87.54	138.34	69.41
$k_{0,2F}$		3.88E+4		1.28E+04		6.90E+03
$E_{a,2F}$		78.67		77.29		71.60
$k_{0,3F}$	3.75E+8	2.62E+4	2.50E+11	1.37E+04	5.53E+12	6.94E+03
$E_{a,3F}$	108.22	76.56	136.52	77.49	138.71	71.56
5-HMF						
$k_{0,1H}$	2.22E+13	2.16E+04	4.83E+15	1.09E+11	2.09E+11	1.47E+01
$E_{a,1H}$	171.96	97.52	176.89	152.49	155.53	71.57
$k_{1,2H}$		1.31E+03		2.20E+09		8.78E+01
$E_{a,2H}$		66.01		126.70		55.79
$k_{0,3H}$	5.08E+19	1.26E+03	9.33E+13	2.31E+09	9.38E+13	3.44E+02
$E_{a,3H}$	207.03	65.82	179.30	126.56	152.77	61.50

In Fig. 7, representative examples of FU and 5-HMF concentrations measured when H, C or L were submitted to hydrothermal treatment at various experimental conditions. In general, model B fitted the experimental data better than model A, thus supporting the existence of side reactions. The corresponding values of E_a and k_0 for each model and each BC are presented in Table 3.

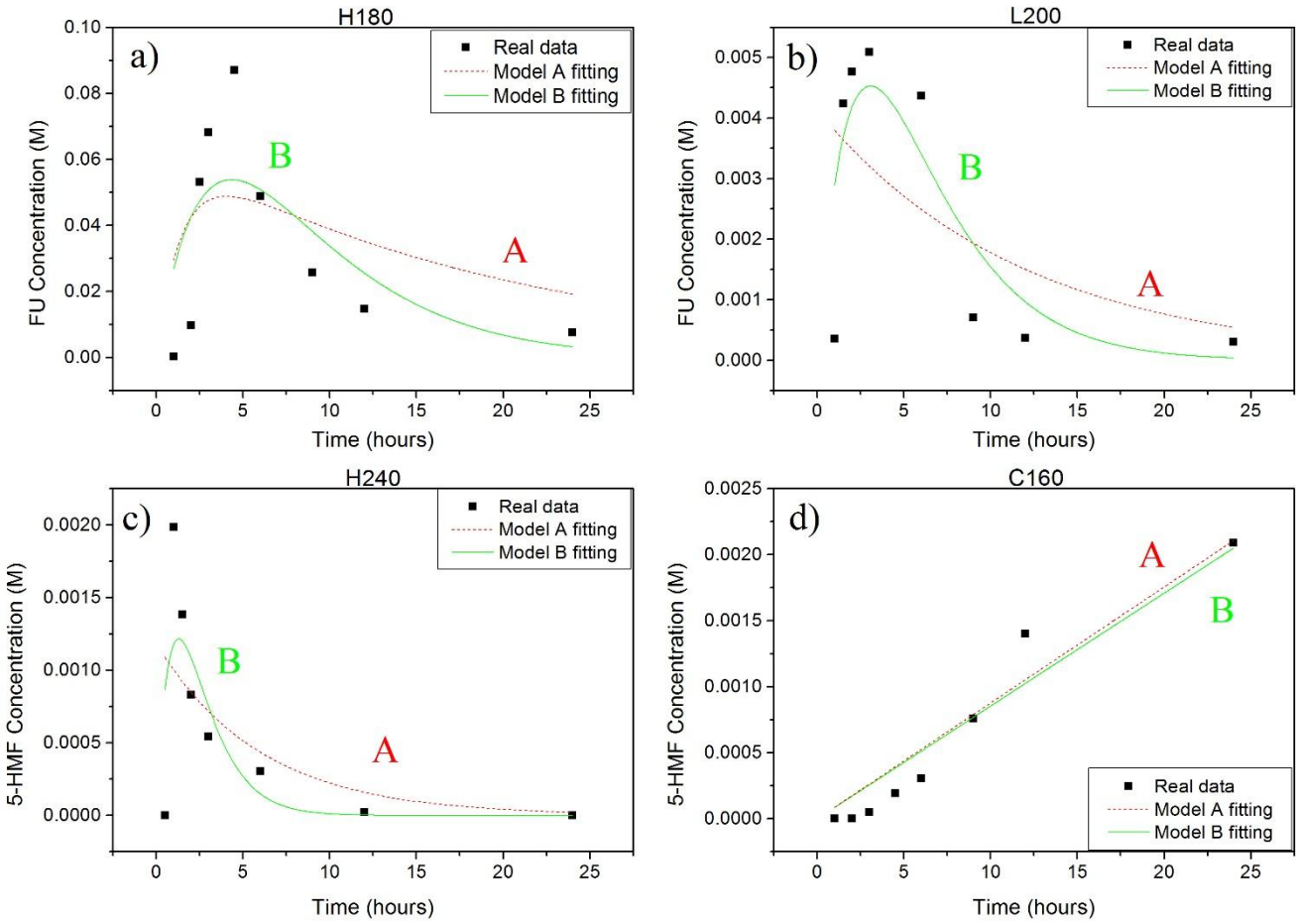

3

Figure 7. Variation of FU (a) and (b) and 5-HMF (c) and (d) concentration with time for a) H submitted at 180 °C, (b) L submitted at 200°C, (c) H submitted at 240 °C, and (d) C submitted at 160°C. Fitting with models A and B to the experimental data are included as dashed and continuous lines, respectively.

Table 4 shows the kinetic parameters reported in the open literature for xylose conversion. These results are compared to those obtained in the present study for hemicellulose, to which model B was applied. Most published works reported higher E_a values than those obtained here (Danon et al., 2014, Liu et al., 2014, Jing and Lü, 2007), which suggests that the effect of temperature observed herein is not as high as that reported in other studies. However, results regarding the same temperature range as in the present work led to lower E_a, thus in agreement with our findings (Kim et al., 2011). Concerning the pre-exponential factors, there is no obvious agreement between the various available results. The reason might be related to the too different ranges of time, temperature or initial concentrations used in this study with respect to those reported in other published works.

Table 4. Activation energies (E_a, kJ mol^{-1}) and pre-exponential factors (k_0, s^{-1}) for xylose conversion into FU (k_1), side products (k_2) and degradation products (k_3) reported herein and in the literature.

Ref	**Catalyst**	**T (ºC)**	k_{1F} **(s^{-1})**		k_{2F} **(s^{-1})**		k_{3F} **(s^{-1})**	
			$k_{0,1F}$ (s^{-1})	$E_{a,1F}$ (kJ·mol^{-1})	$k_{0,2F}$ (s^{-1})	$E_{a,2F}$ (kJ·mol^{-1})	$k_{0,3F}$ (s^{-1})	$E_{a,3F}$ (kJ·mol^{-1})
This study	None	140-240	2.94E+04	85.5	3.89E+04	78.7	1.37E+04	76.56
Danon et al., 2014	HCl & NaCl	160-200	1.05E-03	133.3	2.30E-04	125.8	-	-
Liu et al., 2014	Acetic acid	150-190	9.81E+12	156.6	2.94E+12	149	3.69E+09	115.1
Jing and Lü, 2007	None	180-220	6.28E+06	111.47	1.40E+10	143.14	3.31E+01	58.84
Kim et al., 2011	None	140-240	2.05E+01	76.6	3.31E-1 / 2.66E+12*	58.8 / 154*	4.92E-16	24.2

*Two values are presented since the reaction is a combination between first and second order reaction (first and second values, respectively).

Table 5 shows the kinetic parameters obtained here for cellulose decomposition using model B, compared to those available in the open literature for 5-HMF conversion. E_a values were similar to those previously reported, but k_0 values were lower than those of previous works, probably due, again, to the wider range of temperatures studied in this present work.

Table 5. Activation energies (E_a, kJ mol^{-1}) and pre-exponential factors (k_0, s^{-1}) for hexose conversion into 5-HMF (k_1), side products (k_2) and degradation products (k_3) reported herein and in the literature.

Ref	Raw material	Catalyst	T (ºC)	k_{1H} (s^{-1})		k_{2H} (s^{-1})		k_{3H} (s^{-1})	
				$k_{0,1H}$ (s^{-1})	$E_{a,1H}$ (kJ·mol^{-1})	$k_{0,2H}$ (s^{-1})	$E_{a,2H}$ (kJ·mol^{-1})	$k_{0,3H}$ (s^{-1})	$E_{a,3H}$ (kJ·mol^{-1})
This study	Microcrystalline cellulose	Non catalysed	140-240	1.09E+11	152.49	2.20E+09	126.70	2.31E+09	126.55
Jing and Lü, 2008	Glucose	Non catalysed	180-220	8.44E+07	108.03	7.22E+10	135.71	2.02E+06	95.4
Shen and Wyman 2012	Microcrystalline cellulose	Hydrochloric acid	180-200	4.67E+13*	137	-	-	2.20E+15*	144.83

*Unit of L·(mol·s)$^{-1}$ instead of s^{-1} because proton concentration was not taken into account.

3.6 Phenolic compounds production

Fig. 8 shows the production of nine phenolic compounds obtained by HTC of lignin as a function of severity: 4-hydroxy-3-methoxy benzaldehyde (vanillin), 4-hydroxy-3-methoxy phenylacetone (guaiacyl acetone), 4-hydroxy-3,5-dimethoxy benzaldehyde (syringaldehyde), 2,6-dimethoxyphenol (syringol), 4'-hydroxy-3',5'-dimethoxy acetophenone (acetosyringone), 2-methoxyphenol (guaiacol), phenol, 4-hydroxy-3-methoxyacetophenone (acetovanillone), and 2-methoxy-4-methylphenol (creosol).

Different behaviours can be observed in the investigated range of experimental conditions: vanillin, syringaldehyde and acetosyringone showed a maximum of

concentration, followed by a decrease. Despite the natural scattering of the data, it can be seen that the maximum of vanillin and syringaldehyde production both appeared at a similar severity around 5, whereas the maximum of acetosyringone was reached at a severity close to 6.2. Above such optimal severity values, vanillin and syringaldehyde concentrations dropped significantly whereas that of acetosyringone only decreased moderately. Meanwhile, guaiacyl acetone and acetovanillone presented a linear increase of concentration. Guaiacol, syringol and phenol concentrations also increased, but in a somewhat exponential way. Finally, creosol was only produced at the highest severity, at which its concentration also increased quite fast.

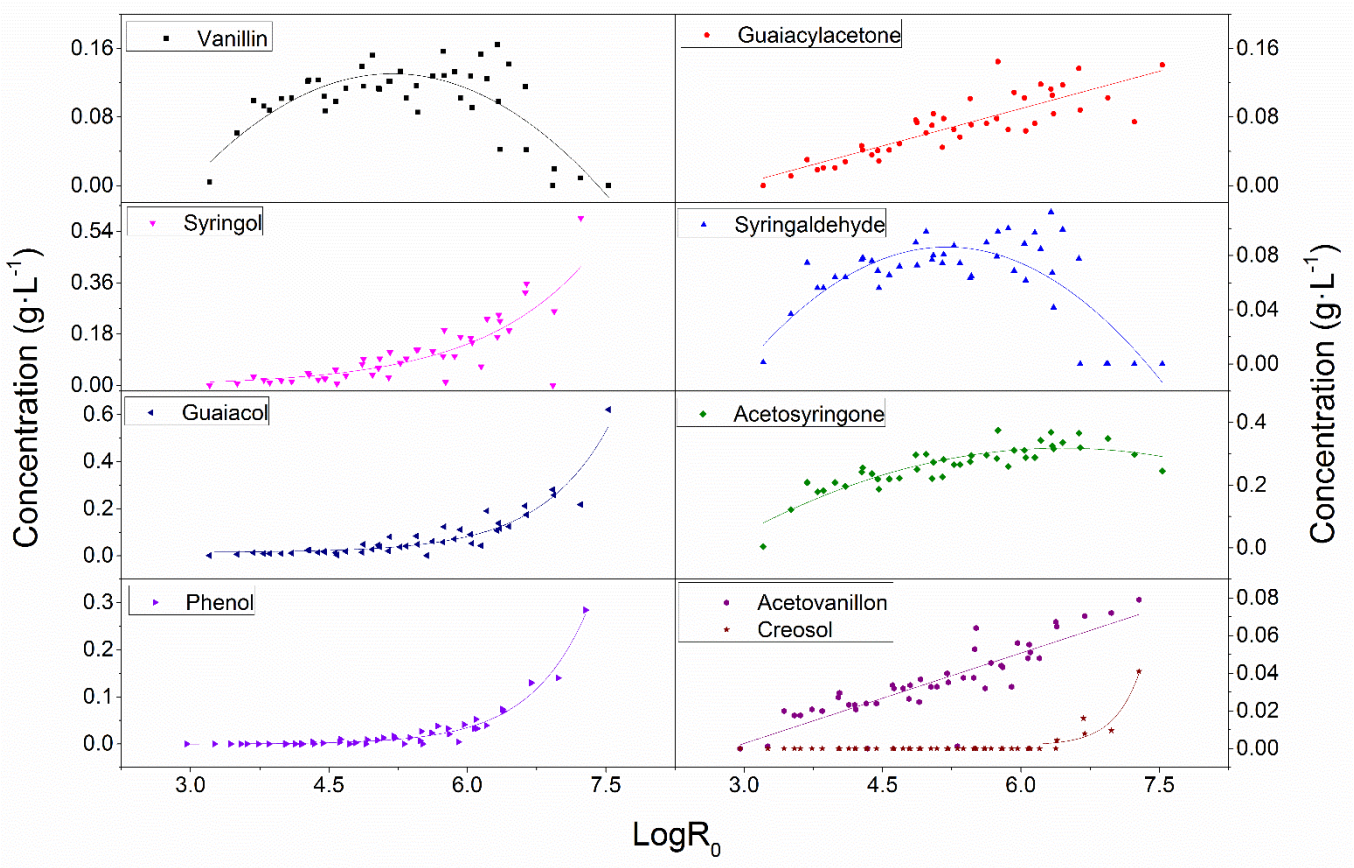

Figure 8. Concentration of the nine phenolic compounds studied in this work as a function of severity.

Regarding the exhibited behaviours, various fitting trends were found whose polynomial, linear or exponential character is accounted for by Eq. (12), (13) and (14), respectively. The values of the corresponding parameters for each compound are given in Table 6, and may be use for predicting the production of phenolic compounds from lignin submitted to hydrothermal treatment at a given severity logR_0.

$$C_{phenolic\ compound} = a + b(logR_0) + c(logR_0)^2 \quad (12)$$

$$C_{phenolic\ compound} = \alpha + \beta(logR_0) \quad (13)$$

$$C_{phenolic\ compound} = \delta + B \cdot e^{(\kappa(logR_0))} \quad (14)$$

Table 6. Parameters from the fits of Eq. (12), (13) or (14) to the data of Fig. 8.

Phenolic Compound	**Parameters of the fits**		
	Polynomial		
	a	*b*	*c*
Vanillin	-0.51	0.26	-0.02
Syringaldehyde	-0.36	0.18	-0.02
Acetosyringone	-0.56	0.28	-0.02
	Linear		
	α		β
Guaiacylacetone	-0.08		0.029
Acetovanillon	-0.05		0.016
	Exponential		
	δ	*B*	κ
Syringol	1.4E-3	0.001	0.851
Guaiacol	0.014	2.87E-5	1.35
Phenol	-6.17E-4	2.27E-6	1.61
Creosol	1.65E-3	1.63E-13	3.58

4. Conclusion

The reactions of cellulose, lignin and hemicellulose submitted to HTC were investigated in a broad range of times and temperatures. The main kinetic parameters were determined, and final pH and hydrochar yield were plotted versus the severity of the process. Hemicellulose and cellulose submitted to HTC produced more acidic

419 solutions containing higher amounts of FU and 5-HMF, respectively, but the latter
420 compounds did not account for the low pH, which was instead due to low molecular-
421 weight acids obtained at the same time.

422 The hydrochar yields increased in the order hemicellulose < cellulose < lignin. The
423 hydrochar yields of cellulose and hemicellulose decreased, around 40%, when the
424 severity increased, and lignin was the most stable compound in the most severe
425 conditions. The amount of liquid fraction recovered after HTC of hemicellulose did not
426 change much with severity, whereas that of cellulose was first stable and then
427 dramatically dropped down to 20%. That of lignin slightly decreased when the severity
428 increased.

429 The kinetics of FU and 5-HMF production were described, using two different
430 models involving consecutive reactions with or without additional side reactions. The
431 pre-exponential factors and activation energies were determined and were comprised
432 within the range of those reported in the open literature. Observed differences were
433 attributed to the broader range of severities used in the present study. Finally, nine
434 phenolic compounds produced by HTC of lignin were also studied, and different
435 behaviours were observed in the range of severities used herein: either a maximum
436 concentration at some optimal severity (vanillin, syringaldehyde and acetosyringone), a
437 continuous linear increase of concentration (guaiacyl acetone and acetovanillone), or a
438 somewhat exponential increase (guaiacol, phenol, syringol and creosol).

439 The present results are expected to be useful for further modelling the behaviour of
440 complex biomass submitted to HTC at various severities. These studies are presently in
441 progress.

442

443

Acknowledgements

The authors gratefully acknowledge the financial support of the CPER 2007–2013 ‘‘Structuration du Pôle de Compétitivité Fibres Grand’Est” (Competitiveness Fibre Cluster, France), through local (Conseil Général des Vosges), regional (Région Lorraine), national (DRRT and FNADT) and European (FEDER, France) funds. This work was also supported by a grant overseen by the French National Research Agency (ANR) as part of the “Investissements d’Avenir” program (ANR-11-LABX-0002-01, Lab of Excellence ARBRE).

References

Basso, D., Weiss-Hortala, E., Patuzzi, F., Castello, D., Baratieri, M., Fiori, L., 2015. Hydrothermal carbonization of off-specification compost: A byproduct of the organic municipal solid waste treatment. Bioresour. Technol. 182, 217–224. https://doi.org/10.1016/j.biortech.2015.01.118

Bergius, F., 1915. Zeitschriftfur komprimierte und flussige gase. pp. 17.

Borrero-López, A.M., Fierro, V., Jeder, A., Ouederni, A., Masson, E., Celzard, A., 2017. High added-value products from the hydrothermal carbonisation of olive stones. Environ. Sci. Pollut. Res. 24, 9859-9869. https://doi.org/10.1007/s11356-016-7807-6

Braghiroli, F.L., Fierro, V., Izquierdo, M.T., Parmentier, J., Pizzi, A., Celzard, A., 2012. Nitrogen-doped carbon materials produced from hydrothermally treated tannin. Carbon 50, 5411–5420. https://doi.org/10.1016/j.carbon.2012.07.027

Braghiroli, F.L., Fierro, V., Izquierdo, M.T., Parmentier, J., Pizzi, A., Celzard, A., 2014. Kinetics of the hydrothermal treatment of tannin for producing carbonaceous microspheres. Bioresour. Technol. 151, 271–277. https://doi.org/10.1016/j.biortech.2013.10.045

Braghiroli, F.L., Fierro, V., Parmentier, J., Vidal, L., Gadonneix, P., Celzard, A., 2015. Hydrothermal carbons produced from tannin by modification of the reaction medium: Addition of H^+ and Ag^+. Ind. Crops Prod. 77, 364–374. https://doi.org/10.1016/j.indcrop.2015.09.010

Braghiroli, F.L., Fierro V., Izquierdo M.T., Parmentier J., Pizzi A., Delmotte L., Celzard A., 2015b. High surface—highly N-doped carbons from hydrothermally treated tannin. Ind. Crops Prod. 66, 282–290. https://doi:10.1016/j.indcrop.2014.11.022

Braghiroli, F.L., Fierro, V., Szczurek, A., Gadonneix, P., Ghanbaja, J., Parmentier, J., Medjahdi, G., Celzard, A., 2017. Hydrothermal treatment of tannin: A route to porous metal oxides and metal/carbon hybrid materials. Inorganics 5, 7. https://doi.org/10.3390/inorganics5010007

Chen, L., Huang, H., Liu, W., Peng, N., Huang, X., 2010. Kinetics of the 5-hydroxymethylfurfural formation reaction in chinese rice wine. J. Agric. Food Chem. 58, 3507–3511. https://doi.org/10.1021/jf904094q

Chen, X., Tao, L., Shekiro, J., Mohaghaghi, A., Decker, S., Wang, W., Smith, H., Park, S., Himmel, M.E., Tucker, M., 2012. Improved ethanol yield and reduced minimum ethanol selling price (MESP) by modifying low severity dilute acid pretreatment with deacetylation and mechanical refining: 1) Experimental. Biotechnol. Biofuels 5, 1–10. https://doi.org/10.1186/1754-6834-5-60

Chen, Z., Zhang, W., Xu, J., Li, P., 2015. Kinetics of xylose dehydration into furfural in acetic acid. Chinese J. Chem. Eng. 23, 659–666. https://doi.org/10.1016/j.cjche.2013.08.003

Chen, X., Lin, Q., He, R., Zhao, X., Li, G., 2017. Hydrochar production from watermelon peel by hydrothermal carbonization. Bioresour. Technol. 241, 236–243. https://doi.org/10.1016/j.biortech.2017.04.012

496 Cross, M.M., 1965. Rheology of non-Newtonian fluids: A new flow equation for
497 pseudoplastic systems. J. Colloid Sci. 20, 417–437.
498 https://doi.org/10.1016/0095-8522(65)90022-X

499 Danon, B., Hongsiri, W., van der Aa, L., de Jong, W., 2014. Kinetic study on
500 homogeneously catalyzed xylose dehydration to furfural in the presence of
501 arabinose and glucose. Biomass Bioenerg. 66, 364–370.
502 https://doi.org/10.1016/j.biombioe.2014.04.007

503 Fang, J., Gao, B., Chen, J., Zimmerman, A.R., 2015. Hydrochars derived from plant
504 biomass under various conditions: Characterization and potential applications
505 and impacts. Chem. Eng. J. 267, 253–259.
506 https://doi.org/10.1016/j.cej.2015.01.026

507 Gao, Y., Wang, X.H., Yang, H.P., Chen, H.P., 2012. Characterization of products from
508 hydrothermal treatments of cellulose. Energy 42, 457–465.
509 https://doi.org/10.1016/j.energy.2012.03.023

510 Girisuta, B., Janssen, L.P.B.M., Heeres, H.J., 2006. A kinetic study on the
511 decomposition of 5-hydroxymethylfurfural into levulinic acid. Green Chem. 8,
512 701-709. https://doi.org/10.1039/b518176c

513 Jatzwauck, M., Schumpe, A., 2015. Kinetics of hydrothermal carbonization (HTC) of
514 soft rush. Biomass Bioenerg. 75, 94–100.
515 https://doi.org/10.1016/j.biombioe.2015.02.006

516 Jing, Q., Lü, X., 2007. Kinetics of non-catalyzed decomposition of D-xylose in high
517 temperature liquid water. Chin. J. Chem. Eng. 15(5), 666-669.
518 https://doi.org/10.1016/S1004-9541(07)60143-8

519 Jing, Q., Lü, X., 2008. Kinetics of non-catalyzed decomposition of glucose in high-
520 temperature liquid water. Chin. J. Chem. Eng. 16, 890–894.
521 https://doi.org/10.1016/S1004-9541(09)60012-4

522 Kang, S., Li, X., Fan, J., Chang, J., 2012. Characterization of hydrochars produced by
523 hydrothermal carbonization of lignin, cellulose, D-xylose, and wood meal. Ind.
524 Eng. Chem. Res. 51, 9023–9031. https://doi.org/10.1021/ie300565d

525 Kim, S.B., Lee, M.R., Park, E.D., Lee, S.M., Lee, H., Park, K.H., Park, M.J., 2011.
526 Kinetic study of the dehydration of D-xylose in high temperature water. React.
527 Kinet. Mech. Catal. 103, 267–277. https://doi.org/10.1007/s11144-011-0320-5

528 Ko, J.K., Kim, Y., Ximenes, E., Ladisch, M.R., 2015. Effect of liquid hot water
529 pretreatment severity on properties of hardwood lignin and enzymatic hydrolysis
530 of cellulose. Biotechnol. Bioeng. 112, 252–262.
531 https://doi.org/10.1002/bit.25349

532 Liu, H., Hu, H., Mojtaba, M., Jahan, M.S., 2014. Kinetics of furfural production from
533 pre-hydrolysis liquor (PHL) of a kraft-based hardwood dissolving pulp
534 production process. Biomass Bioenerg. 66, 320–327.
535 https://doi.org/10.1016/j.biombioe.2014.02.003

536 Lu, X., Pellechia, P.J., Flora, J.R. V, Berge, N.D., 2013. Influence of reaction time and
537 temperature on product formation and characteristics associated with the
538 hydrothermal carbonization of cellulose. Bioresour. Technol. 138, 180–190.
539 https://doi.org/10.1016/j.biortech.2013.03.163

Lynam, J.G., Coronella, C.J., Yan, W., Reza, M.T., Vasquez, V.R., 2011. Acetic acid and lithium chloride effects on hydrothermal carbonization of lignocellulosic biomass. Bioresour. Technol. 102, 6192–6199. https://doi.org/10.1016/j.biortech.2011.02.035

Marcotullio, G., Tavares Cardoso, M.A., De Jong, W., Verkooijen, A.H.M., 2009. Bioenergy II: Furfural destruction kinetics during sulphuric acid-catalyzed production from biomass. Int. J. Chem. React. Eng. 7. https://doi.org/10.2202/1542-6580.1980

Marcotullio, G., 2011. The chemistry and technology of furfural production in modern lignocellulose-feedstock biorefineries. Delft University of Technology, Netherlands.

Onwudili, J.A., 2015. Influence of reaction conditions on the composition of liquid products from two-stage catalytic hydrothermal processing of lignin. Bioresour. Technol. 187, 60–69. https://doi.org/10.1016/j.biortech.2015.03.088

Overend, R.P., Chornet, E., 1987. Fractionation of lignocellulosics by steam-aqueous pretreatments. Philos. Trans. R. Soc. Lond. 321, 523–536. https://doi.org/10.1098/rsta.1987.0029

Perez, R.F., Fraga, M.A., 2014. Hemicellulose-derived chemicals: One-step production of furfuryl alcohol from xylose. Green Chem. 16, 3942–3950. https://doi.org/10.1039/c4gc00398e

Pińkowska, H., Wolak, P., Złocińska, A., 2011. Hydrothermal decomposition of xylan as a model substance for plant biomass waste - Hydrothermolysis in subcritical water. Biomass Bioenerg. 35, 3902–3912. https://doi.org/10.1016/j.biombioe.2011.06.015

Rasmussen, H., Sørensen, H.R., Meyer, A.S., 2014. Formation of degradation compounds from lignocellulosic biomass in the biorefinery: Sugar reaction mechanisms. Carbohydr. Res. 385, 45–57. https://doi.org/10.1016/j.carres.2013.08.029

Reza, M.T., Becker, W., Sachsenheimer, K., Mumme, J., 2014. Hydrothermal carbonization (HTC): Near infrared spectroscopy and partial least-squares regression for determination of selective components in HTC solid and liquid products derived from maize silage. Bioresour. Technol. 161, 91–101. https://doi.org/10.1016/j.biortech.2014.03.008

Reza, M.T., Rottler, E., Herklotz, L., Wirth, B., 2015. Hydrothermal carbonization (HTC) of wheat straw: Influence of feedwater pH prepared by acetic acid and potassium hydroxide. Bioresour. Technol. 182, 336–344. https://doi.org/10.1016/j.biortech.2015.02.024

Selmi, T., Sanchez-Sanchez, A., Gadonneix, P., Jagiello, J., Seffen, M., Sammouda, H., Celzard, A., Fierro, V., 2018. Tetracycline removal with activated carbons produced by hydrothermal carbonisation of Agave americana fibres and mimosa tannin. Ind. Crops Prod. 115, 146–157. https://doi.org/10.1016/j.indcrop.2018.02.005

Shen, J. Wyman, C.E., 2012. Hydrochloric acid-catalyzed levulinic acid formation from cellulose: Data and kinetic model to maximize yields. AIChE J. 58 (1), 236–246. https://doi.org/10.1002/aic.12556

585 Steinbeiss, S., Gleixner, G., Antonietti, M., 2009. Effect of biochar amendment on soil
586 carbon balance and soil microbial activity. Soil Biol. Biochem. 41, 1301–1310.
587 https://doi.org/10.1016/j.soilbio.2009.03.016

588 Wang, Y., Yang, R., Li, M., Zhao, Z., 2015. Hydrothermal preparation of highly porous
589 carbon spheres from hemp (Cannabis sativa L.) stem hemicellulose for use in
590 energy-related applications. Ind. Crops Prod. 65, 216–226.
591 https://doi.org/10.1016/j.indcrop.2014.12.008

592 Xu, J., Chen, Y., Cheng, J.J., Sharma-Shivappa, R.R., Burns, J.C., 2011. Delignification
593 of switchgrass cultivars for bioethanol production. BioResources 6, 707–720.
594 https://doi.org/10.15376/biores.6.1.707-720

595 Yang, G., Pidko, E.A., Hensen, E.J.M., 2012. Mechanism of Bronsted acid-catalyzed
596 conversion of carbohydrates. J. Catal. 295, 122–132.
597 https://doi.org/10.1016/j.jcat.2012.08.002

598 Yemiş. O., Mazza, G., 2012. Optimization of furfural and 5-hydroxymethylfurfural
599 production from wheat straw by a microwave-assisted process. Bioresour.
600 Technol. 109, 215–223. https://doi.org/10.1016/j.biortech.2012.01.031

601 Zeitsch, K.J., 2000. The chemistry and technology of furfural and its many by-products,
602 volume 13, first ed. Elsevier, Amsterdam.

603 Zhou, X.F., 2014. Conversion of kraft lignin under hydrothermal conditions. Bioresour.
604 Technol. 170, 583–586. https://doi.org/10.1016/j.biortech.2014.08.076